Does leaf shedding protect stems from cavitation during seasonal droughts? A test of the hydraulic fuse hypothesis

Brett T. Wolfe[1,2], John S. Sperry[1] and Thomas A. Kursar[1,2]

[1]Department of Biology, University of Utah, Salt Lake City, UT 84112, USA; [2]Smithsonian Tropical Research Institute, PO Box 0843-03092, Balboa, Ancon, Panama

Author for correspondence:
Brett T. Wolfe
Tel: +507 6437 6537
Email: btwolfe@gmail.com

Received: *9 March 2016*
Accepted: *1 June 2016*

New Phytologist (2016) **212:** 1007–1018
doi: 10.1111/nph.14087

Key words: drought deciduousness, hydraulic limitation, hydraulic segmentation hypothesis, leaf abscission, leaf phenology, seasonally dry tropical forest, xylem cavitation.

Summary

- During droughts, leaves are predicted to act as 'hydraulic fuses' by shedding when plants reach critically low water potential (Ψ_{plant}), thereby slowing water loss, stabilizing Ψ_{plant} and protecting against cavitation-induced loss of stem hydraulic conductivity (K_s).
- We tested these predictions among trees in seasonally dry tropical forests, where leaf shedding is common, yet variable, among species. We tracked leaf phenology, Ψ_{plant} and K_s in saplings of six tree species distributed across two forests.
- Species differed in their timing and extent of leaf shedding, yet converged in shedding leaves as they approached the Ψ_{plant} value associated with a 50% loss of K_s and at which their model-estimated maximum sustainable transpiration rate approached zero. However, after shedding all leaves, the Ψ_{plant} value of one species, *Genipa americana*, continued to decline, indicating that water loss continued after leaf shedding. K_s was highly variable among saplings within species and seasons, suggesting a minimal influence of seasonal drought on K_s.
- Hydraulic limits appear to drive diverse patterns of leaf shedding among tropical trees, supporting the hydraulic fuse hypothesis. However, leaf shedding is not universally effective at stabilizing Ψ_{plant}, suggesting that the main function of drought deciduousness may vary among species.

Introduction

Trees must allow water to evaporate from their leaves (i.e. transpire) in order to maintain the CO_2 uptake that supplies photosynthesis. This water is held under tension in a 'tug of war' within the soil–plant–atmosphere continuum (Sperry *et al.*, 2002). As water moves down gradients of water potential, plant water potential (Ψ_{plant}) must remain below soil water potential (Ψ_{soil}) for water uptake to feed the transpiration stream. However, as Ψ_{soil} and Ψ_{plant} decrease, hydraulic conductance within the soil–canopy continuum decreases as a result of cavitation within soil pore spaces and xylem conduits. These two processes result in a constraint, such that trees must regulate their transpiration rate (E) below the critical level (E_{crit}) above which soil–canopy conductance reaches zero and complete 'hydraulic failure' occurs. On short timescales, stomata act as valves to control E and Ψ_{plant} (Sperry *et al.*, 2002). However, as Ψ_{soil} decreases, E_{crit} decreases and, at some point, E_{crit} reaches zero, when any amount of transpiration would cause hydraulic failure. As closed stomata may leak and as water evaporates from leaf cuticles, additional water-conserving responses enhance survival during droughts (Levitt, 1972).

The hydraulic segmentation hypothesis states that, during droughts, the most peripheral plant organs (e.g. leaves) experience the lowest water potential; therefore, if their vulnerability to cavitation is the same as or greater than that of more central organs (e.g. the main stem or bole), the peripheral organs will cavitate before the central organs (Zimmermann, 1983; Tyree *et al.*, 1993; Tyree & Zimmermann, 2002). As cavitation lowers hydraulic conductivity, this response would retain water within the central organs, protecting them from cavitation. Moreover, as cavitation renders the peripheral organs non-functional, the hydraulic segmentation hypothesis also predicts that these organs may be shed or abscised (Tyree *et al.*, 1993). In theory, this hydraulic architecture is adaptive because central organs are more costly than peripheral organs for plants to replace. Thus, leaves are predicted to act as 'hydraulic fuses' that break the soil–plant–atmosphere continuum by shedding before stems incur damage, either through local hydraulic failure or at some point before failure by hydraulic stress-induced senescence (Tyree & Sperry, 1988; Tyree *et al.*, 1993). Although the role of stomatal control has received much attention (Klein, 2014), the role of leaf shedding in the context of the hydraulic fuse hypothesis has rarely been tested (Tyree *et al.*, 1993).

Seasonally dry tropical forests contain many tree species that shed some or all of their leaves during annual dry seasons (Axelrod, 1966; Frankie *et al.*, 1974; Condit *et al.*, 2000). In these ecosystems, leaf shedding during drought (i.e. drought deciduousness) may represent a critical response that protects stems as predicted by the hydraulic fuse hypothesis. However, despite its potential importance, the hydraulic function of leaf shedding in tropical plants is poorly understood (Brodribb *et al.*, 2002). It is also intriguing that the timing, rate and extent of leaf shedding vary considerably among species (Bullock & Solis-Magallanes, 1990; Williams *et al.*, 2008). Such diversity suggests multiple physiological mechanisms for the avoidance of drought-induced mortality. If the hydraulic fuse hypothesis is correct and if leaf shedding is a drought response that protects stems from hydraulic failure, diverse leaf phenologies correspond to divergence among species in hydraulic limits within the soil–canopy continuum. For example, the stems of deciduous species may be more vulnerable to cavitation than those of co-occurring evergreen species. However, this simple prediction has received equivocal support. Some studies have found no difference in vulnerability to cavitation between deciduous and evergreen species (Machado & Tyree, 1994; Sobrado, 1997; Brodribb *et al.*, 2002; Markesteijn *et al.*, 2011), whereas others have found higher vulnerability in deciduous species than in evergreen species (Brodribb *et al.*, 2003; Choat *et al.*, 2005; Lopez *et al.*, 2005; Fu *et al.*, 2012). This suggests that the role of leaf shedding in the maintenance of hydraulic systems of tropical trees deserves a closer mechanistic analysis.

In order to address how leaf shedding relates to the regulation of Ψ_{plant} and to the avoidance of stem hydraulic failure, we tracked saplings in two seasonally dry tropical forests for leaf phenology, stomatal conductance, Ψ_{plant} and stem hydraulic conductivity. We focused on saplings because they are amenable to canopy measurements. In addition, because saplings have relatively high mortality during droughts (Enquist & Enquist, 2011), their physiology strongly influences the identity of the species that dominate the forest canopy. We combined our census data with additional measurements of stem vulnerability to cavitation to parameterize a hydraulic model that predicts E_{crit} in given environmental conditions. We then tested the following predictions of the hydraulic fuse hypothesis: the timing of leaf shedding coincides with key points of hydraulic stress (e.g. E_{crit} near zero); leaf shedding stabilizes Ψ_{plant} during seasonal droughts; and saplings maintain stable stem hydraulic conductivity during seasonal droughts.

Materials and Methods

Study sites and species

This study was conducted in two seasonally dry forests in Panama. One forest, the Parque Natural Metropolitano (8°59′N, 79°32′W), is transitional between moist and dry forest (‘transitional forest’), with annual rainfall of 1800 mm. The other forest, the Eugene Eisenmann Reserve (8°31′N, 79°53′W), is a dry forest, with annual rainfall of 1590 mm. Both are mature secondary forests and experience dry seasons from mid-December to May. We measured rainfall in the dry forest with an automated rain gauge (Onset Corp., Bourne, MA, USA) and obtained data from the transitional forest from the Smithsonian Tropical Research Institute. In each forest, we placed a temperature and relative humidity sensor (models HMP50 and CS500; Campbell Scientific, Logan, UT, USA) in the understory (50 cm height). Air temperature and relative humidity were measured every 10 min and hourly mean temperature and minimum and maximum relative humidity were recorded on CR200 data loggers (Campbell Scientific). In general, the dry season in the dry forest is slightly longer, hotter and higher in vapor pressure deficit (VPD) than in the transitional forest. The two dry seasons encompassed by the study (2012 and 2013) fit this pattern, except that the 2013 dry season in the transitional forest extended for *c.* 30 d longer than normal (Fig. 1i,j; see Supporting Information Table S1). Late in the dry seasons, we measured Ψ_{soil} in profiles at each site (Fig. S1). Ψ_{soil} was lower in the dry forest than in the transitional forest (e.g. in 2013, Ψ_{soil} values at 50 cm depth were -4.6 ± 0.7 and -2.1 ± 0.9 MPa (mean ± SD) in the dry and transitional forest, respectively). In each forest, we chose four tree species that were common as saplings and that were reported to vary in deciduousness and wood density as adults (Table 1). Two species were shared between the forests, and so six species were studied in total. Throughout the text, the study species are referred to by genus name.

Censuses of leaf area, stomatal conductance and plant water potential

Ten healthy-looking saplings of each species were selected for censuses of leaf area and stomatal conductance (g_s). Mean ± SD basal diameter ranged among species from 7.2 ± 2.7 mm to 27.3 ± 16.8 mm (Table S2). Censuses were conducted every 3–6 wk from November 2011 to July 2013, more often during the dry seasons. In the transitional forest, three *Cojoba*, one *Cavanillesia* and one *Annona* died, all after November 2012, reducing their sample sizes towards the end of the study. On each census plant, the positions of the leaves along the stems were noted and the length of each leaf was measured to the nearest 1 mm with a ruler. For compound-leaved species (Table 1), the length of the most distal leaflet was measured and the number of leaflets on each leaf was counted. In each census, the presence or absence of previously measured leaves and the number of leaflets were recorded, and any newly produced leaves were measured for length and number of leaflets. Leaves that were incompletely expanded during a census were re-measured for length in the subsequent census.

For each species, 23–94 leaves were collected from nearby saplings and measured for leaf area with an LI-3100 area meter (Li-Cor Biosciences, Lincoln, NE, USA). The relationship between leaf length and area was modeled with simple linear regression on log-transformed values, including number of leaflets as a cofactor for compound-leaved species (Fig. S2). These models were used to estimate the area of each census leaf, the values of which were summed to obtain the total leaf area of each sapling in each census.

During each census, three leaves on each sapling were randomly selected and measured for g_s with a porometer (LI-1600; Li-Cor Biosciences) between 10:00 and 14:00 h. As leaves were not amphistomatic, g_s was measured on the abaxial (lower) side. If saplings had fewer than three leaves during a census, all leaves were measured. The porometer's cuvette was maintained at < 70% relative humidity to reduce measurement error (McDermitt, 1990). Measurements were made within 60 s of placing the cuvette over

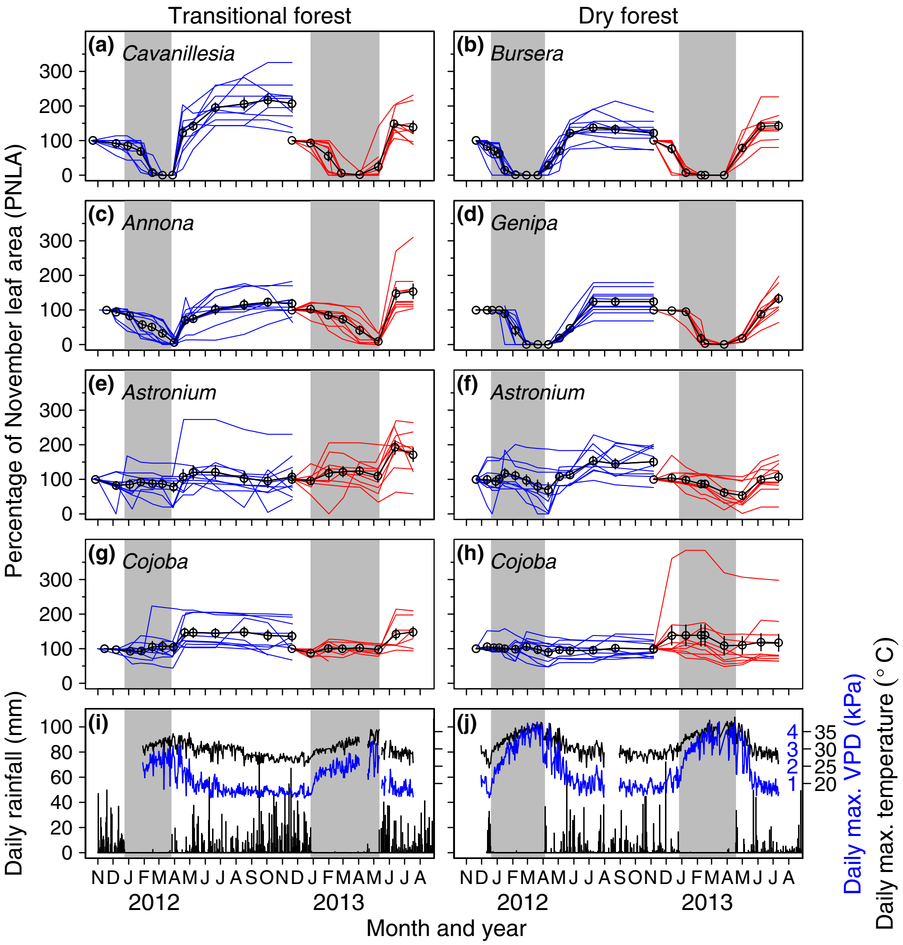

Fig. 1 Time course of (a–h) percentage leaf area (relative to November leaf area, PNLA) among saplings of six tree species and (i, j) weather in two seasonally dry tropical forests. Dry seasons are shaded in grey. In (a–h), PNLA for individual saplings is represented by blue and red lines for the first and second census years, respectively. Black circles represent means (± SE). Note that, for the second census year, we set leaf area as 100% in November 2012. In (i, j), bars represent daily rainfall, black lines represent daily maximum temperature and blue lines represent daily maximum vapor pressure deficit (VPD).

Table 1 Study species traits, descriptions of adult leaf phenology (Pérez, 2008) and adult wood density (S. J. Wright, unpublished)

Species	Family	Leaf shape	Adult leaf phenology	Adult wood density (g cm^{-3})
Annona hayesii Saff. in Standl.	Annonaceae	Simple	Not reported	0.50
Astronium graveolens Jacq.	Anacardiaceae	Compound	Deciduous	0.82
Bursera simaruba (L.) Sarg.	Burseraceae	Compound	Deciduous	0.43
Cavanillesia platanifolia (Bonpl.) Kunth	Malvaceae	Simple	Deciduous	0.19
Cojoba rufescens (Benth.) Britton and Rose	Fabaceae	Compound	Semi-deciduous	0.69
Genipa americana L.	Rubiaceae	Simple	Deciduous	0.69

the leaf to avoid affecting g_s. The porometer was regularly calibrated with a dew point generator (LI-610; Li-Cor Biosciences).

At each census, four saplings of each species located within 50 m of the saplings measured for leaf area and g_s were measured for leaf water potential (Ψ_{leaf}). Most saplings were measured for Ψ_{leaf} in only one census; otherwise saplings were left at least 5 months between measurements. At predawn (04:00–06:30 h) and midday (11:00–14:00 h), two leaves were collected from each sapling, sealed in humidified plastic bags, placed in a cooler with ice and measured for Ψ_{leaf} with a pressure chamber < 2 h after collection. Ψ_{leaf} for each sapling was taken as the average of the two leaves. When plants were leafless, terminal twigs were collected to measure twig water potential (Ψ_{twig}) following the same protocol as for Ψ_{leaf}, except that Ψ_{twig} was measured only at predawn. Comparisons with psychrometric measurements of Ψ_{twig} confirmed that the pressure chamber measurements accurately assessed Ψ_{twig} (Wolfe & Kursar, 2015). As water potential is under a gradient within transpiring plants, we took the mean of Ψ_{leaf} at predawn and midday to represent Ψ_{plant} for each sapling in each census.

Hydraulic conductivity and vulnerability to cavitation

We searched the area near the census plants (*c.* 2 ha) for healthy-looking saplings (110–400 cm tall) to measure for stem hydraulic conductivity. During the 2012 wet season (July–December) and during the subsequent dry season (March–April 2013), eight saplings of each species were collected (four at predawn and four at midday, $n = 128$). For the three species that flushed leaves near the onset of the wet season (*Cavanillesia*, *Bursera* and *Genipa*; Fig. 1), we also collected eight saplings (four at predawn and four at midday, $n = 24$) that were flushing leaves at the onset of the 2013 wet season (May). For collection, the saplings were cut near the base with pruning shears, sealed in opaque plastic bags humidified with wet paper towels and brought to the laboratory. Additional saplings were collected during the 2012 and 2014 wet seasons and bench dried to assess vulnerability to cavitation. They were air dried in the laboratory for 2–300 h and then re-bagged for 2 h before subsequent measurements ($n = 101$, 9–16 per species in each forest).

In the laboratory, Ψ_{leaf} was measured with a pressure chamber on three leaves and averaged. Stem water potential (Ψ_{stem}) was assumed to equal Ψ_{leaf} because sealing of the stems in opaque bags stopped transpiration (however, see Tobin *et al.* (2013) for a case in which this method may have failed at low Ψ_{stem}). For saplings that were leafless, we measured Ψ_{stem} as described earlier for Ψ_{twig} of leafless census plants.

The stem was submerged in tap water and a segment of 30 cm in length was removed with pruning shears. We ensured that the stem length between the end cut in the field and the segment measured for hydraulic conductivity was longer than the maximum vessel length (Table S3). The ends of the segment were recut with a fresh razor and the bark within 2 cm of the ends was removed. The segment was attached to a hydraulic conductivity apparatus (Sperry *et al.*, 1988) that measured flow rates with graduated pipettes and perfused with filtered (0.1 μm) and degassed 10 mM KCl. To correct for passive water uptake, flow rates were measured under four pressure heads, in the range 0.98–8.6 kPa, and hydraulic conductivity was calculated as the slope of the regression of the flow rate on the pressure gradient across the stem segment (Torres-Ruiz *et al.*, 2012). Stem area-specific hydraulic conductivity (K_s) was calculated by dividing conductivity by the segment's cross-sectional area. The cross-sectional area was calculated by averaging two diameter measurements made with calipers (to 0.1 mm) on each end of the segment.

Vulnerability to cavitation was assessed as the decrease in K_s with decreasing Ψ_{stem}. A three-parameter Weibull function was fitted as:

$$K_s = a \times \exp(-(-\Psi_{stem}/b)^c), \qquad \text{Eqn 1}$$

through all K_s measurements for each species. As multiple factors limit K_s independently of Ψ_{stem} at which K_s is measured (e.g. previous drought stress, pathogen attack, stem bending), we fitted regressions through the 90th quantile of the measurements, which represents the upper limit of K_s as a function of Ψ_{stem} (Cade & Noon, 2003). We fitted the regressions with the R package quantreg (Koenker, 2013). The Weibull functions were used to calculate Ψ_{stem} at 50% and 80% loss of K_s (Ψ_{50} and Ψ_{80}, respectively).

It has been reported recently that the excision of stem segments for K_s measurements while the xylem is under tension produces artifactually low K_s values for some species (Wheeler *et al.*, 2013; but see Venturas *et al.*, 2015). As our initial K_s measurements were liable to this excision artifact, for the measurements made in 2014, we relaxed the xylem tension by sequentially cutting back the stems towards the K_s segment while the stem was under water. The values of K_s from 2014 did not differ from the earlier measurements (visual inspection, Fig. 2), and so we included the full dataset in our analyses.

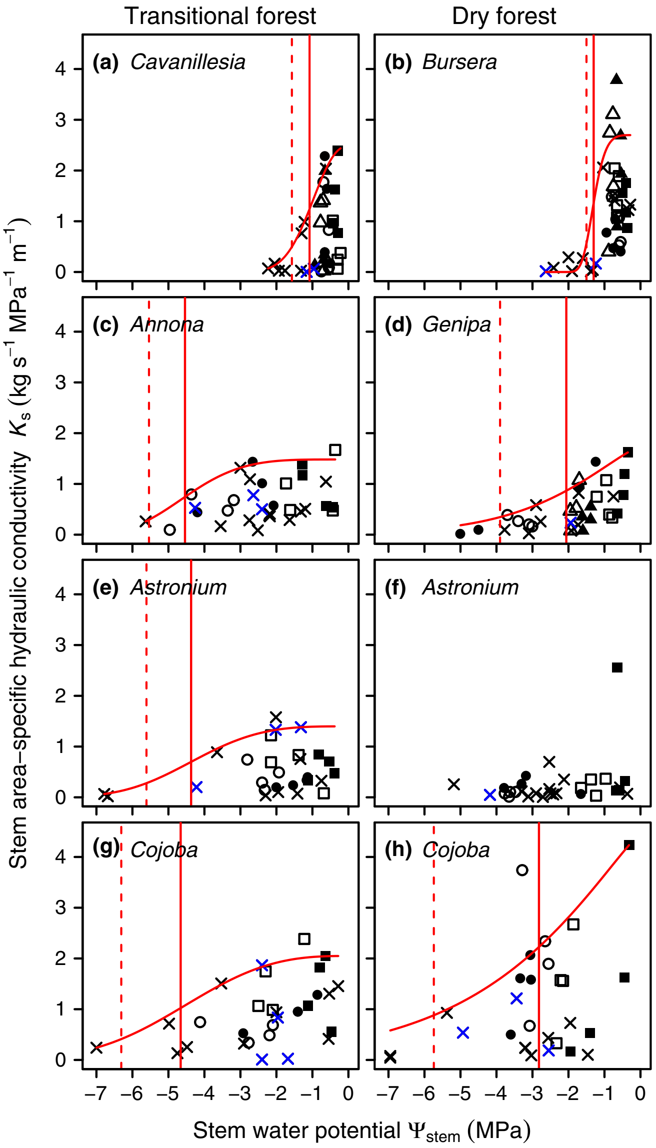

Fig. 2 Stem area-specific hydraulic conductivity (K_s) as a function of stem water potential (Ψ_{stem}) for (a–h) saplings of six tree species distributed across two forests. Squares, circles and triangles represent samples collected during the wet and dry seasons, and during early wet season leaf flushing, respectively. Closed and open symbols represent samples collected during predawn and midday, respectively. Crosses represent samples collected during the wet season and bench dried before measurement of Ψ_{stem} and K_s. Blue crosses represent samples in which xylem tension was relaxed before excising the K_s segment in order to test for an excision artifact (see the Materials and Methods section). Vulnerability to cavitation was assessed as the 90th quantile regression with a Weibull function (Eqn 1), drawn as red lines. Regression coefficients are listed in Supporting Information Table S4. At the Ψ_{stem} values at which the regression predicts 50% loss of K_s (Ψ_{50}) and 80% loss of K_s (Ψ_{80}), vertical solid and dashed lines are drawn, respectively. A regression could not be fitted to the data in (f).

To test whether K_s varied seasonally and diurnally, we set up a two-way ANOVA for each species with season, time of day (predawn vs midday) and their interaction as fixed effects. Linear contrasts were used to compare K_s between seasons and between times of day within a season. The false discovery rate method of Benjamini & Hochberg (1995) was used to correct for multiple comparisons to $\alpha = 0.05$.

Relationships among leaf shedding, stomatal conductance and vulnerability to cavitation

In order to test for relationships between leaf shedding and Ψ_{plant}, we first calculated the percentage of leaf area relative to the November censuses preceding the dry seasons (PNLA) for each sapling. The November censuses were used as reference points (PNLA = 100%) because that is when most saplings had maximum leaf area (Fig. 1). We then calculated the mean PNLA for each species in each census and used standardized major axis regression to assess its relationship with Ψ_{plant} within each census year (first year, November 2011–August 2012; second year, November 2012–July 2013). To compare among species for sensitivity of leaf shedding in response to Ψ_{plant}, we calculated the Ψ_{plant} value at which PNLA was 50% (LA_{50}; analogous to the Ψ_{50} value for sensitivity of K_s to Ψ_{stem}).

Similarly, we tested for relationships between g_s and Ψ_{plant}. We took the mean g_s for each species at each census and plotted it against Ψ_{plant}. Then, for each census year, we fitted a Weibull function through the points with nonlinear regression. Using the intercept of the regression as the maximum g_s, we calculated the Ψ_{plant} value at which g_s was 50% of the maximum (SC_{50}). We then tested whether leaf responses (SC_{50} and LA_{50}) were correlated with points of hydraulic stress in the stem (Ψ_{50} and Ψ_{80}) among species using Pearson's correlation analysis.

Hydraulic failure parameters

For each census date, we used a soil–plant–atmosphere model to estimate the percentage loss of hydraulic conductance in the stem network (PLC_{stem}) vs in the total soil–canopy path (PLC_{total}), and the critical transpiration rate (E_{crit}) above which PLC_{total} would go to 100%. The model was developed by Sperry *et al.* (1998) and upgraded to include stomatal control of E and Ψ_{leaf} (Sperry & Love, 2015; Sperry *et al.*, 2016). The model calculates the steady-state relationship of E vs Ψ_{leaf} (and hence E_{crit}) from Ψ_{soil} and vulnerability curves that describe the decline in soil and plant hydraulic conductance with Ψ. E predictions assume that E is increasingly limited, as negative Ψ_{soil} and high VPD would otherwise drive the plant closer to E_{crit}. The plant therefore exploits, but does not exceed, the available water transport capacity as limited by E_{crit}. Only when low Ψ_{soil} drives E_{crit} to zero is PLC_{total} predicted to reach 100%. As details of the model have been described elsewhere (Sperry & Love, 2015; Sperry *et al.*, 2016), here we describe its application.

The model was run for each species–site combination, inputting the time series of paired Ψ_{soil} and midday VPD across all censuses. Ψ_{soil} was set to predawn Ψ_{leaf}. Midday VPD was set to the ambient value measured concurrently with g_s. The model predicted the corresponding time series of midday Ψ_{leaf}, whole-canopy diffusive conductance (G, $G = E/\text{VPD}$, $\text{kg h}^{-1}\text{ m}^{-2}$ basal area), E_{crit}, PLC_{stem} and PLC_{total}. The model was tuned to obtain the best fit to measured G and Ψ_{leaf}, thus maximizing its accuracy for the prediction of E_{crit} and PLC. The measured G was calculated for each census plant and date by multiplying g_s by the leaf area of the canopy and dividing by the stem basal area.

Our stem vulnerability curves (Table S4) were used to represent the plant and Van Genuchten's (1980) equation for the soil-to-root (rhizosphere) component. The required soil texture parameters were obtained from Leij *et al.* (1996) for top-horizon soils observed within 200 m of the census plants (clay in transitional forest, sandy clay loam in dry forest; B. L. Turner, pers. comm.). To predict PLC_{stem}, we had to input the maximum (no embolism) hydraulic conductance of the stem network. The default stem conductance was set to 25% of the soil–canopy resistance (roots at 50%, leaves at 25%). The 50–50 root–shoot division appears roughly consistent among woody plants (Sperry *et al.*, 1998), as is the 25% value for leaves (Sack & Tyree, 2005). However, the leaf component can shift with plant size (Von Allmen *et al.*, 2015), and so we assessed the consequences of varying the 25–25 stem–leaf breakdown from 20–30 to 30–20.

The model was fitted by iteratively adjusting three unknown inputs: maximum soil–canopy hydraulic conductance (k_{max}), maximum G (G_{max}) and the average percentage rhizosphere hydraulic resistance. The latter input is the extent to which soil–root hydraulic conductance limits plant water uptake. The lower the surface area of absorbing roots vs leaves, the more 'vulnerable' is the Van Genuchten soil hydraulic function relative to the plant's vulnerability curve, and the greater the percentage rhizosphere resistance. The rhizosphere adjustment can also compensate for missing vulnerability curve information from the plant, in our case the lack of root and leaf vulnerability curves. Missing root or leaf curves prevent us from predicting PLC in these organs, but we can still predict E_{crit}, PLC_{total} and PLC_{stem}, which was sufficient for our purposes. The k_{max}, G_{max} and percentage rhizosphere resistance were iterated manually to maximize the r^2 of a single regression through normalized values (i.e. divided by their respective observed average for each species–site combination across the censuses) for measured vs modeled G and Ψ_{leaf}. The best fits were obtained by running the model in irreversible mode where PLC in xylem is permanent (vs reversible mode where PLC in xylem is fully and instantly reversible; Sperry & Love, 2015).

If leaf shedding is a response to diminishing transport capacity and acts to maintain stem K_s, as predicted by the hydraulic fuse hypothesis, leaf shedding should be closely associated with drought levels that drive E_{crit} to zero. To test this, we plotted PNLA as a function of E_{crit} and used nonlinear regression to fit Weibull functions through the points for each census year. To test the prediction that leaf shedding slows water loss rates through reduced hydraulic conductance, we plotted the model's output of $\text{PLC}_{\text{total}}$ as a function of measured PNLA, and used nonlinear regression to fit a function of the form:

$$\text{PLC}_{\text{total}} = b - \exp(\text{PNLA}/a) \qquad \text{Eqn 2}$$

Finally, to test whether the saplings regulated Ψ_{plant}, such that the loss of hydraulic conductance in the stem was low compared with that of more peripheral plant components, we plotted PLC_{stem} against $\text{PLC}_{\text{total}}$.

Results

Seasonal changes in leaf area, stomatal conductance and water potential

In both the transitional and dry forests, species exhibited a wide range of dry season deciduousness (Fig. 1). *Cavanillesia* and *Bursera* saplings shed their leaves early during the dry seasons (Fig. 1a,b), whereas, at the other extreme, *Cojoba* saplings did not reduce their leaf area during the dry seasons in either forest (Fig. 1g,h). To varying degrees, the other species were intermediate in deciduousness: *Genipa* shed its leaves later than *Bursera* and remained leafless for 2 months (Fig. 1d); *Annona* shed its leaves gradually through the dry season, but flushed new leaves within days of shedding the old ones (Fig. 1c); *Astronium* maintained its leaf area during the dry season in the transitional forest, but shed nearly 50% of its leaf area in the dry forest (Fig. 1e,f). These patterns were similar between the 2012 and 2013 dry seasons.

All species in both forests had lower g_s during the dry season than during the wet season (Fig. S3). Deciduous species reduced g_s before shedding leaves. *Astronium* and *Cojoba* had lower dry season g_s in the dry forest than in the transitional forest (Fig. S3).

Among species, there was a wide range in seasonal patterns of Ψ_{plant} (Fig. S4). *Cavanillesia* and *Bursera* maintained Ψ_{plant} above −1 MPa throughout the dry seasons. At the other extreme, *Genipa* reached −6.5 MPa during the 2012 dry season and −4.3 MPa during the 2013 dry season. Meanwhile, *Annona*, *Astronium* and *Cojoba* had lower Ψ_{plant} during the dry season than during the wet season. *Astronium* and *Cojoba* reached lower Ψ_{plant} in the dry forest than in the transitional forest (Fig. S4).

Stem hydraulic conductivity and vulnerability to cavitation

We found a wide range of Ψ_{50} and Ψ_{80} values among species (Fig. 2). For *Astronium* in the dry forest, K_s was generally low, irrespective of Ψ_{stem} (Fig. 2f); as a Weibull function, or any function, did not fit these data, this population was excluded from the analyses that included vulnerability to cavitation. K_s did not differ significantly between predawn and midday for any species in any season (Fig. 3). K_s differed significantly between seasons in only two cases: *Cojoba* in the transitional forest had lower K_s in the dry season than in the wet season, and *Bursera* had lower K_s in the dry season than during leaf flush at the onset of the wet season (linear contrasts, $P < 0.05$; Fig. 3).

Coordination between drought responses and vulnerability to cavitation among species

Within species, g_s generally decreased as Ψ_{plant} decreased during both dry seasons (Fig. S5). However, during 2012, the nonlinear regressions for *Cavanillesia* and *Bursera* did not converge on a Weibull function, apparently because the saplings had a wide range in g_s throughout the relatively small range in Ψ_{plant} (Fig. S5). As these species probably had a threshold response that

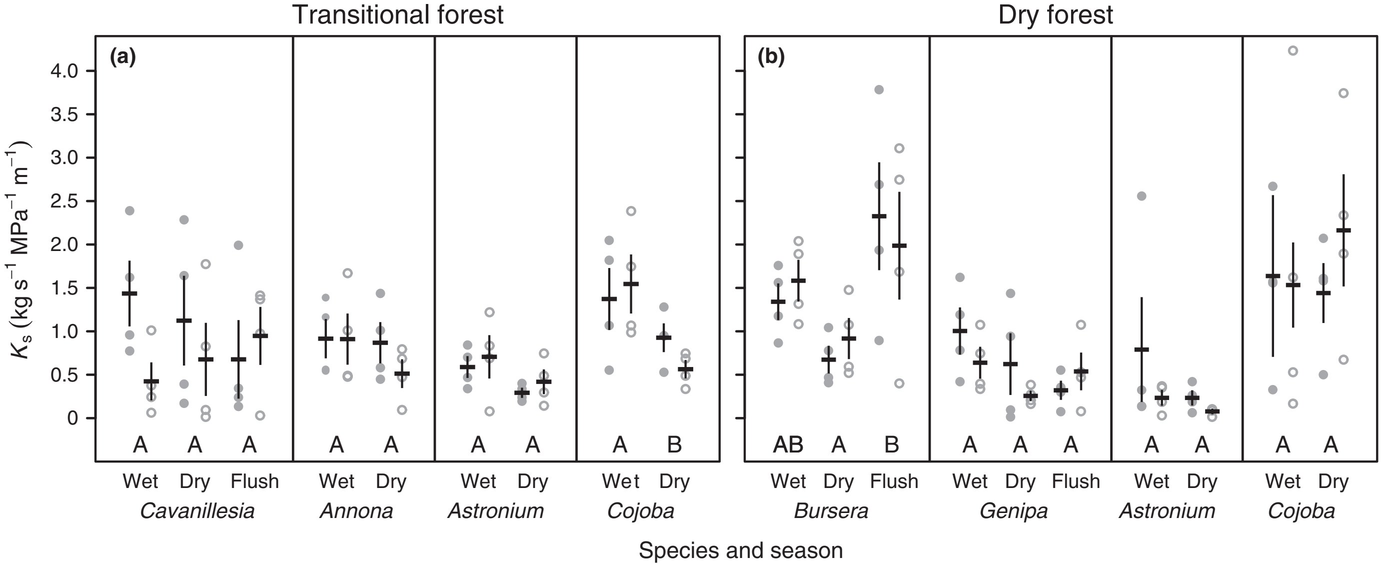

Fig. 3 Stem area-specific hydraulic conductivity (K_s) among seasons and time of day within season for (a) four species in a transitional forest and (b) four species in a dry forest. Closed and open circles represent measurements from predawn and midday, respectively. Bars represent mean ± SE. Wet, dry and flush are the wet season, dry season and during early wet season leaf flushing, respectively. Seasons that share letters are not significantly different. Within season, no differences were detected between predawn and midday.

could not be fitted via regression, we used the minimum Ψ_{plant} as an estimate of SC_{50} for *Cavanillesia* and *Bursera* during 2012. As for g_s, PNLA generally decreased as Ψ_{plant} decreased (Fig. 4; Table S5). However, in the dry forest during 2013, *Cojoba* had higher PNLA at lower Ψ_{plant} (Fig. 4h), because it added leaf area in the late wet season and early dry season, then lost leaf area near the onset of the wet season (Fig. 1h). As *Cojoba* in the dry forest never reached LA_{50} in 2013, we excluded this datum from the LA_{50} correlation analyses. In general, species had similar SC_{50}, LA_{50} and minimum Ψ_{plant} values between the 2012 and 2013 dry seasons (Fig. 5). Among species, lower SC_{50} and LA_{50} were correlated with lower Ψ_{50} and Ψ_{80} in both census years (Fig. 5a–d). Minimum Ψ_{plant} was not correlated with Ψ_{50} or Ψ_{80} during either census year (Fig. 5e,f).

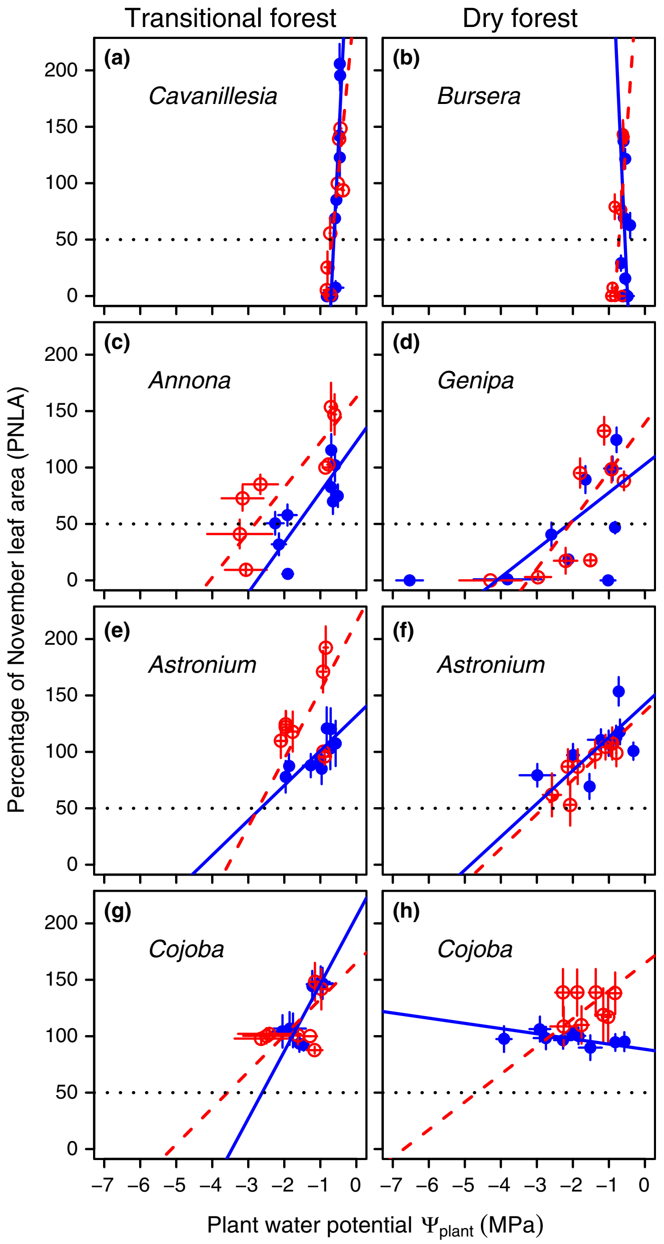

Fig. 4 Percentage of leaf area (relative to November leaf area, PNLA) as a function of plant water potential (Ψ_{plant}; mean of predawn and midday leaf or leafless twig water potential) for (a–h) six species distributed across two seasonally dry tropical forests (see Figs 1 and Supporting Information S4). Closed blue and open red circles represent means (± SE) for censuses within the first and second census years (2012 and 2013), respectively. Standardized major axis regressions are shown with solid blue and dashed red lines for the first and second years, respectively. Regression coefficients are listed in Table S5. The Ψ_{plant} value at which the leaf area reached 50% (LA_{50}) was calculated as the point at which the regression line intersects 50% PNLA (dotted lines).

Hydraulic limits to gas exchange

The hydraulic model successfully fitted the wide swings in measured G and Ψ_{leaf} during the 2 yr of measurement in six of the

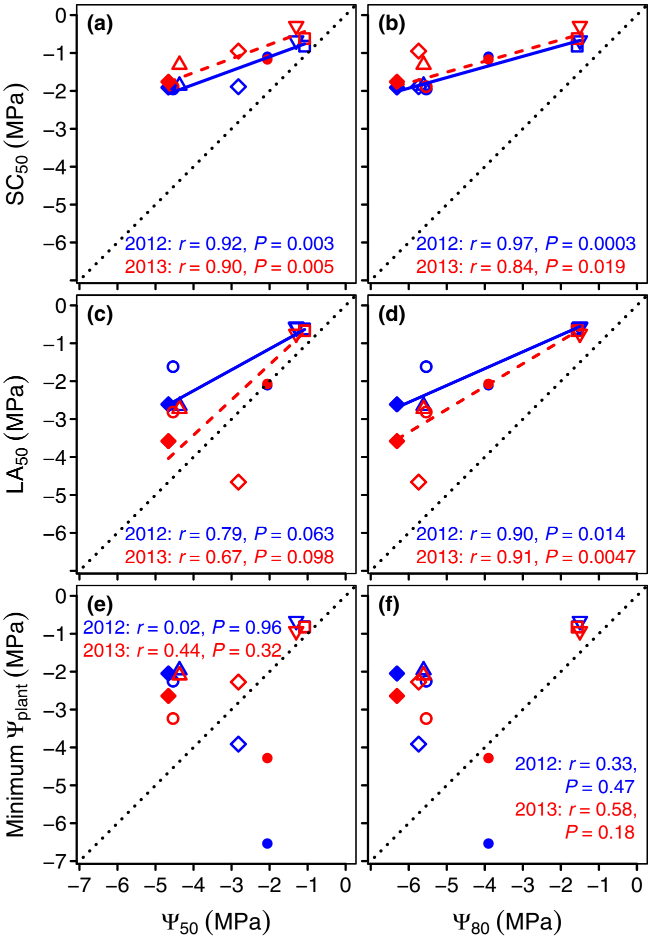

Fig. 5 Correlations between the stem water potential associated with 50% and 80% loss of hydraulic conductivity (Ψ_{50} and Ψ_{80}, respectively) and (a, b) the plant water potential (Ψ_{plant}) at which stomatal conductance is 50% of maximum (SC_{50}), (c, d) the Ψ_{plant} value at which the leaf area is 50% of the November census before the dry season (LA_{50}), and (e, f) the minimum Ψ_{plant} value reached during the dry season. Species are represented as: *Annona*, open circle; transitional forest *Astronium*, up-pointed triangle; *Bursera*, down-pointed triangle; *Cavanillesia*, open square; transitional forest *Cojoba*, closed diamond; dry forest *Cojoba*, open diamond; *Genipa*, closed circle. Blue and red symbols represent values obtained in the first and second years of the census (2012 and 2013), respectively. When Pearson's correlation coefficient was $P < 0.10$ (statistics shown in each panel), the standardized major axis regression line is drawn as a solid blue or dashed red line for 2012 and 2013, respectively. Dotted 1 : 1 lines are shown for reference.

seven cases (Figs S6, S7). Excluding the poor fit to *Bursera*, the average r^2 was 0.79 (range, 0.62–0.94) for G (modeled vs measured) and 0.74 (0.38–0.94) for Ψ_{leaf}. The reasonable model fit to G and Ψ_{leaf} resulted in reasonable estimates of E_{crit}, $\mathrm{PLC}_{\mathrm{stem}}$ and $\mathrm{PLC}_{\mathrm{total}}$ (Table S6 lists the mean absolute errors of model outputs). Outputs were insensitive to the assumed contribution of stems to continuum resistance: a 20–30% range resulted in < 1% change in E/E_{crit} and $\mathrm{PLC}_{\mathrm{stem}}/\mathrm{PLC}_{\mathrm{total}}$ (Table S7). The average percentage rhizosphere resistance required to achieve the model fit was consistently high (64–86% excepting *Bursera*, Table S8), indicating either a strong soil limitation or compensation for unknown root and leaf vulnerability.

The poor fit for *Bursera* was caused by the unusual result of midday Ψ_{leaf} being *less* negative than Ψ_{soil}. This happened during the dry seasons when *Bursera* was essentially leafless. The model cannot predict reverse Ψ gradients, and so, for *Bursera*, it was unable to explain the variation in Ψ_{leaf} with statistical significance (Fig. S7). Because PLC predictions are Ψ dependent, we did not use them for *Bursera*. However, the model predicted a significant 53% of the variation in G for this species (Fig. S6), and so we accepted E and E_{crit} outputs for *Bursera*.

Hydraulic limitations within all species were predicted to reduce E during the dry seasons, from maxima of 1.6–14.3 kg h^{-1} m^{-2} to minima of 0.34–2.7 kg h^{-1} m^{-2} (Fig. 6a). PNLA approached zero (full deciduousness) only near the lowest values of E_{crit}, 0.5–2 kg h^{-1} m^{-2} (Fig. 6b), supporting the prediction that leaf shedding is associated with E_{crit} approaching zero. The relationship between PNLA and E_{crit} was similar between the two dry seasons (F test, $P = 0.15$; Table S9). $\mathrm{PLC}_{\mathrm{total}}$ predicted by the model was related to the measured PNLA such that, at PNLA > 80% (only slight leaf loss), $\mathrm{PLC}_{\mathrm{total}}$ was not yet severe, < 60%. With greater leaf loss, at PNLA < 60%, $\mathrm{PLC}_{\mathrm{total}}$ increased only slightly (Fig. 6c; Table S10). As a result, measured leaf area reached zero before complete loss of modeled water transport capacity. All species reached relatively high values of $\mathrm{PLC}_{\mathrm{total}}$ during the dry seasons, with *Genipa* reaching the highest (range of 73–97% excluding *Genipa*; *Genipa* = 99.4%), yet $\mathrm{PLC}_{\mathrm{stem}}$ remained relatively low in all species except *Genipa* (range of 5–62% excluding *Genipa*; *Genipa* = 84%; Fig. 6d).

Discussion

We found distinct patterns of leaf phenology within each species and population (Fig. 1). Although species fit within ‘evergreen’ and ‘deciduous’ functional groups (evergreen, *Astronium* and *Cojoba*; deciduous, *Cavanillesia*, *Bursera*, *Annona* and *Genipa*), this grouping misses important differences among species. For example, in the transitional forest, *Cavanillesia* reached zero leaf area *c.* 5 wk earlier than *Annona*. These phenological differences are probably linked to physiological and morphological differences among species and probably influence species performance. The quantification of deciduousness among populations, such as

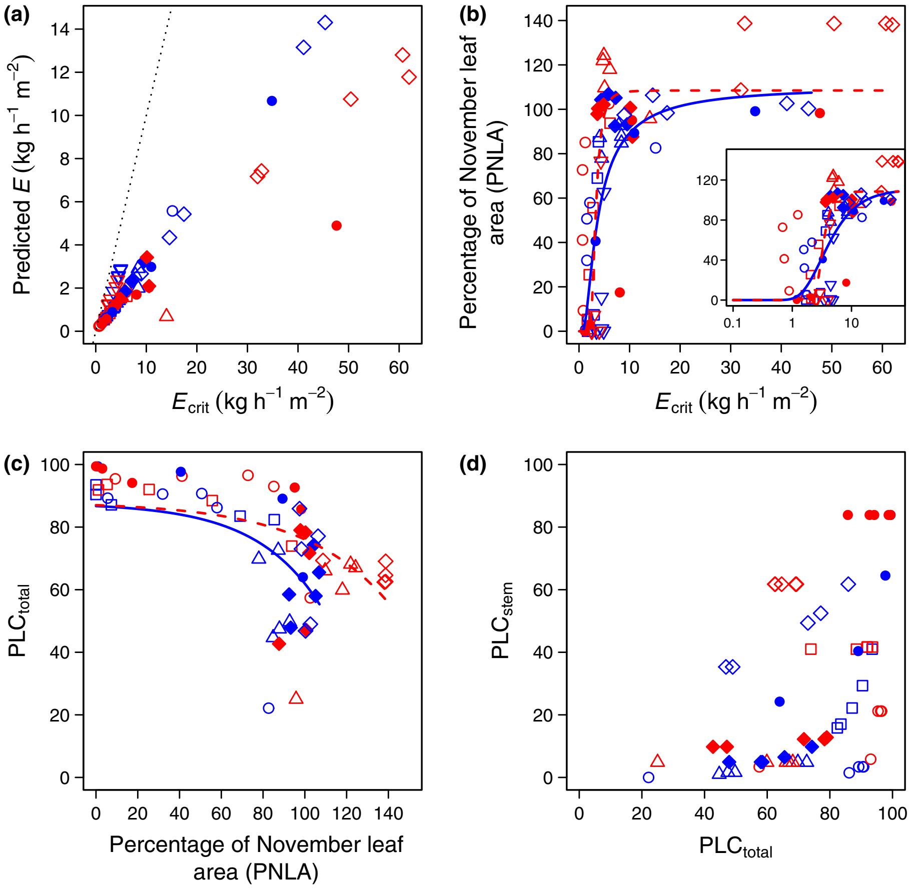

Fig. 6 Relationships among modeled hydraulic parameters and measured percentage leaf area (relative to November leaf area, PNLA). (a) Model-predicted transpiration rate (E) as a function of the transpiration rate that would cause hydraulic failure in the soil–canopy continuum (E_{crit}). (b) PNLA as a function of E_{crit}. (c) Modeled percentage loss of hydraulic conductance in the whole soil–canopy continuum ($\mathrm{PLC}_{\mathrm{total}}$) as a function of PNLA. (d) Modeled percentage loss of hydraulic conductance in the stem ($\mathrm{PLC}_{\mathrm{stem}}$) as a function of $\mathrm{PLC}_{\mathrm{total}}$. Blue and red symbols represent values from censuses within the dry seasons (i.e. within the shaded regions in Fig. 1) of the first and second years of the census (2012 and 2013), respectively. Species are represented as: *Annona*, open circle; transitional forest *Astronium*, up-pointed triangle; *Bursera*, down-pointed triangle; *Cavanillesia*, open square; transitional forest *Cojoba*, closed diamond; dry forest *Cojoba*, open diamond; *Genipa*, closed circle. In (a), the dotted 1 : 1 line is shown for reference. In (b, c), nonlinear regression lines are drawn as solid blue and dashed red lines for the 2012 and 2013 dry seasons, respectively. The inset in (b) shows PNLA as a function of E_{crit} with the x-axis on a log scale.

the time lag between the onset of the dry season and leaf loss, may be more informative than grouping (Méndez-Alonzo *et al.*, 2012). However, we found that the assessment of leaf shedding as a function of Ψ_{plant} and E_{crit} (Figs 4, 6) helped to elucidate the mechanisms underlying the diverse patterns of deciduousness among tropical trees.

Leaf shedding occurs at key points of hydraulic stress

We found that PNLA decreased precipitously when E_{crit} was reduced to $< 5\ \mathrm{kg\ h^{-1}\ m^{-2}}$ (Fig. 6b). Likewise, LA_{50} was correlated with Ψ_{50} and Ψ_{80} among species (Fig. 5c,d). LA_{50} was above the 1 : 1 line with Ψ_{50}, indicating that saplings shed half of their leaf area before they experienced levels of cavitation that can lead to hydraulic failure in their stems. Similar effects have been reported for potted seedlings of Mexican dry forest tree species, among which Ψ_{plant} at 80% leaf loss was correlated with Ψ_{80} (Pineda-García *et al.*, 2013). Taken together, these results suggest that hydraulic limits drive a universal pattern of leaf shedding among juvenile trees in seasonally dry tropical forests.

Most of the decrease in measured leaf area (from 100% to 0% PNLA) was associated with the increase in model-estimated PLC_{total} from 60% to 85% (Fig. 6c). As we did not directly parameterize vulnerability to cavitation in the rhizosphere, roots or leaves, we cannot predict their contribution to the soil–canopy bottleneck that drives PLC_{total} higher as the dry season progresses. Although a high soil limitation was required to fit the model (via high percentage rhizosphere resistance, Table S8), this could be compensating for the unknown vulnerability of roots and leaves (which are typically more vulnerable than stems, see references within Sperry & Love, 2015). Regardless, the prediction of $PLC_{total} >> PLC_{stem}$ as the dry season progresses (Fig. 6d) is consistent with the hydraulic fuse hypothesis – the loss of hydraulic conductance associated with leaf shedding occurred only after major declines in hydraulic conductance other than in the stems. Indeed, most leaf shedding occurred when PLC_{total} approached levels that were associated with dieback and tree mortality (i.e. 60–90%; Sperry & Love, 2015).

Although leaf shedding was associated with hydraulic stress, we found no evidence that it was associated with hydraulic failure; E remained below E_{crit} for all species (Fig. 6). As hydraulic failure before leaf shedding would impede nutrient resorption (Marchin *et al.*, 2010), trees adapted to seasonally dry conditions may be programmed to senesce and abscise leaves before hydraulic failure occurs. Leaves on our study trees commonly turned yellow or red before shedding (B. T. Wolfe, pers. obs.), which suggests that senescence occurred (Munné-Bosch & Alegre, 2004). How environmental conditions, such as drought and light, interact with endogenous factors, such as leaf age, to induce senescence is still poorly understood (Munné-Bosch & Alegre, 2004; Giraldo & Holbrook, 2011; Schippers *et al.*, 2015). Various models predict that the optimal time for leaf senescence occurs as net CO_2 assimilation becomes unfavorable (reviewed by Givnish, 2002). Others predict that leaf senescence occurs in response to water stress, such as a loss of hydraulic conductance in petioles (Tyree *et al.*, 1993; Brodribb *et al.*, 2003). These models are essentially indistinguishable under natural drought conditions because water stress, stomatal closure and the resultant reduced net CO_2 assimilation co-occur. However, when droughts are out of season or extreme, leaves may act as hydraulic fuses without a senescence–abscission response. For example, during extreme droughts, leaves attached to stems that experience high losses in K_s are often described as turning brown on the stem or abscising while green, suggesting that a loss of K_s inhibits leaf senescence (Marchin *et al.*, 2010; Nardini *et al.*, 2013).

From our censuses, we cannot discern whether our 'evergreen' species would shed leaves under drought conditions in which their E_{crit} was closer to zero and, conversely, whether our 'deciduous' species would maintain leaves under less intense droughts. Studies that manipulate water availability in seasonally dry forests should address these issues. One such study, on Barro Colorado Island (BCI), Panama, found that dry season irrigation did not affect leaf shedding in canopy trees of 16 out of 19 species, despite effectively raising Ψ_{leaf} (Wright & Cornejo, 1990). However, most canopy trees on BCI access soil water (i.e. high E_{crit}) during the relatively mild dry season, such that leaf shedding phenology is probably driven by leaf production, which coincides with the dry season peak in irradiance (Wright & van Schaik, 1994). By contrast, when 1-yr-old seedlings near BCI were irrigated during the dry season, leaf shedding was significantly reduced in 25 of 28 species (Engelbrecht & Kursar, 2003). Probably, the effect of irrigation was stronger for seedlings because unirrigated seedlings have poor dry season soil water access. Together, these results suggest that, when E_{crit} approaches zero, water stress overrides irradiance as a driver of leaf phenology.

Leaf shedding may not stabilize Ψ_{plant} during seasonal droughts

During both dry seasons, Ψ_{plant} of *Genipa* declined even after saplings shed all of their leaves, putting them at risk of hydraulic failure (i.e. $\Psi_{plant} < \Psi_{80}$; Figs 5f, S4). In contrast with dynamic failure caused by $E > E_{crit}$, this would be static failure (*sensu* Tyree & Sperry, 1988), in which Ψ_{stem} and K_s decline without a significant xylem pressure gradient produced by transpiration. Although a reduction in the evaporative surface area through leaf shedding certainly slows water loss, the pattern exhibited by *Genipa* does not support a central prediction of the hydraulic fuse hypothesis – that leaf shedding protects stems from hydraulic stress. Similarly, after adult trees of several species in Costa Rican dry forests shed all of their leaves, they experienced stem diameter contraction associated with water loss (Daubenmire, 1972; Reich & Borchert, 1984).

Although *Cavanillesia* and *Bursera* had stable Ψ_{plant} after shedding leaves, they also had relatively stable Ψ_{plant} during the onset of the dry season, before shedding leaves (Fig. S4). These species have high stem hydraulic capacitance that maintains high Ψ_{plant}, even with significant water loss (Wolfe & Kursar, 2015). For *Cavanillesia*, direct measurements of stem water content revealed no difference between the wet and dry seasons, suggesting that leaf shedding contributed to the complete retention of stem water

(Wolfe & Kursar, 2015). Meanwhile, *Bursera* had significantly lower stem water content in the dry season than in the wet season, suggesting that either leaf shedding did not stop water loss or that water loss occurred before leaf shedding (Wolfe & Kursar, 2015), and so it is unclear whether leaf shedding retained stem water. By contrast, *Annona* had Ψ_{plant} that decreased at the onset of the dry season, before the saplings shed leaves, and then stabilized after leaf shedding (compare Figs 1c and S4c). This pattern suggests that leaf shedding was effective at stopping water loss in *Annona*.

The effectiveness of leaf shedding in stopping water loss depends on several factors that were not measured. For example, the permeability of the stem surface to water vapor would affect the rate at which leafless stems lose water. This trait probably varies widely among tropical tree species, considering the great diversity of bark traits (Rosell *et al.*, 2014). Likewise, low root radial hydraulic conductance would help to maintain $\Psi_{\text{plant}} > \Psi_{\text{soil}}$ by slowing the rate at which water diffuses from roots to dry soil. Root radial hydraulic conductance is highly dynamic on timescales of minutes to hours through aquaporin regulation (Javot & Maurel, 2002), and on longer timescales through mechanisms such as root shrinkage (Nobel & Cui, 1992) and suberization (Lo Gullo *et al.*, 1998). In order for leaf shedding to stop water loss from trees rooted in dry soil, it must be coordinated with root responses. The lack of correlation between minimum Ψ_{plant} and Ψ_{50} or Ψ_{80} among species (Fig. 5e,f) could reflect differences among species in this coordination.

Do saplings maintain stable K_s during normal dry seasons?

Throughout the dry season, for all species except *Genipa*, the modeled PLC_{stem} remained at < 65%, whereas $\text{PLC}_{\text{total}}$ reached 73–97% (Fig. 6d). This result is consistent with the hydraulic segmentation hypothesis, in that stem hydraulic conductance was protected from cavitation relative to the more peripheral components. For most species, the model predictions of low PLC_{stem} concurred with direct measurements of K_s, which did not vary between the wet and dry seasons (Fig. 3). The model prediction of 84% PLC_{stem} in *Genipa* appears contradictory to direct measurements, where K_s did not vary between seasons (Figs 3b, 6d). However, unlike the other species, some field-collected (not bench-dried) *Genipa* saplings indeed reached $\Psi_{\text{stem}} < \Psi_{80}$, whereas the *Genipa* saplings that maintained near-wet season K_s also maintained near-wet season Ψ_{stem} (Fig. 2). On average, the K_s saplings maintained higher dry season water potential than the census saplings used to parameterize Ψ_{soil} in the model (2013 census, mean ± SE: -3.2 ± 0.4 vs -4.3 ± 1.1 MPa), possibly because they were larger (Tables S2, S3). Taller saplings were necessary to prevent cavitation in the K_s segments during collection (Table S3). Thus, both field measurements and model predictions suggest that the census saplings that reached lower Ψ_{plant} experienced high PLC_{stem}. Considering that none of the *Genipa* census saplings died during the study, this species probably possesses mechanisms to recover K_s, either through embolism refilling or xylem production.

We are aware of only one other study from the tropics with comparable seasonal K_s measurements (Sobrado, 1993). Two other studies that measured K_s across seasons are not comparable because petioles were included in the K_s segments (Brodribb *et al.*, 2002) or the segments were rehydrated before K_s measurements (Ishida *et al.*, 2010), precluding inferences of seasonal change in native K_s within stems. Sobrado (1993) found that, within distal branch segments of adult trees in a Venezuelan dry forest, four deciduous species had 65–92% lower K_s in the dry season than in the wet season, whereas two evergreen species did not have significantly lower K_s. Thus, the deciduous species in the study of Sobrado (1993) lost more K_s than the saplings in our study (Figs 3, 4). The results of Sobrado (1993) do not support the prediction that leaf shedding protects stems from hydraulic stress, yet it is unclear whether leaf shedding preceded or followed the loss of K_s. As native K_s is considered to be a key factor affecting drought performance and survival (McDowell *et al.*, 2013), more studies should address the conditions, traits and behaviors that are associated with changes in K_s during (seasonal) droughts.

Conclusions

Among species in seasonally dry tropical forests, diverse patterns of leaf phenology coincide in that leaf shedding occurs as saplings reach hydraulic limits that reduce E_{crit} (and, by extension, CO_2 assimilation) to near zero. This is consistent with the prediction that leaf shedding is cued to occur before leaves are cut off from their water source through hydraulic failure, although the cues remain unclear. The extension of this relationship to adult trees could improve leaf phenology parameters in terrestrial biosphere models (Powell *et al.*, 2013). However, our results and those of others suggest that leaf shedding does not always stop water loss or the loss of K_s in stems, contrary to the predictions of the hydraulic fuse hypothesis. Rather than drought deciduousness acting universally as a water conservation strategy, its main function (or 'ultimate cause') may vary among species and situations, acting as a means for respiration reduction, nutrient re-utilization and leaf-to-root area balancing.

Acknowledgements

B.T.W. was supported by a short-term fellowship from the Smithsonian Tropical Research Institute, a University of Utah (UU) Graduate Research Fellowship, a UU Global Change and Sustainability Center grant and a National Science Foundation (NSF) GK-12 Program fellowship from the UU's Think Globally Teach Locally Program. Funding was provided by NSF grant DEB-0444590 to T.A.K. We thank Joe Wright for advice and support, Sarah Bruemmer for laboratory assistance, and Parque Natural Metropolitano and Eugene Eisenmann Reserve for study site access.

Author contributions

B.T.W., J.S.S. and T.A.K. designed the experiment. B.T.W. conducted the field and laboratory work. B.T.W. and J.S.S. analyzed the data. B.T.W., J.S.S. and T.A.K. wrote the manuscript.

References

Axelrod DI. 1966. Origin of deciduous and evergreen habits in temperate forests. *Evolution* 20: 1–15.

Benjamini Y, Hochberg Y. 1995. Controlling the false discovery rate: a practical and powerful approach to multiple testing. *Journal of the Royal Statistical Society: Series B (Methodological)* 57: 289–300.

Brodribb TJ, Holbrook NM, Edwards EJ, Gutiérrez MV. 2003. Relations between stomatal closure, leaf turgor and xylem vulnerability in eight tropical dry forest trees. *Plant, Cell & Environment* 26: 443–450.

Brodribb TJ, Holbrook NM, Gutiérrez MV. 2002. Hydraulic and photosynthetic co-ordination in seasonally dry tropical forest trees. *Plant, Cell & Environment* 25: 1435–1444.

Bullock SH, Solis-Magallanes JA. 1990. Phenology of canopy trees of a tropical deciduous forest in Mexico. *Biotropica* 22: 22–35.

Cade BS, Noon BR. 2003. A gentle introduction to quantile regression for ecologists. *Frontiers in Ecology and the Environment* 1: 412–420.

Choat B, Ball MC, Luly JG, Holtum JAM. 2005. Hydraulic architecture of deciduous and evergreen dry rainforest tree species from North-Eastern Australia. *Trees – Structure and Function* 19: 305–311.

Condit R, Watts K, Bohlman SA, Perez R, Foster RB, Hubbell SP. 2000. Quantifying the deciduousness of tropical forest canopies under varying climates. *Journal of Vegetation Science* 11: 649–658.

Daubenmire R. 1972. Phenology and other characteristics of tropical semi-deciduous forest in north-western Costa Rica. *Journal of Ecology* 60: 147–170.

Engelbrecht BMJ, Kursar TA. 2003. Comparative drought-resistance of seedlings of 28 species of co-occurring tropical woody plants. *Oecologia* 136: 383–393.

Enquist BJ, Enquist CAF. 2011. Long-term change within a Neotropical forest: assessing differential functional and floristic responses to disturbance and drought. *Global Change Biology* 17: 1408–1424.

Frankie GW, Baker HG, Opler PA. 1974. Comparative phenological studies of trees in tropical wet and dry forests in the lowlands of Costa Rica. *Journal of Ecology* 62: 881–919.

Fu P-L, Jiang Y-J, Wang A-Y, Brodribb TJ, Zhang J-L, Zhu S-D, Cao K-F. 2012. Stem hydraulic traits and leaf water-stress tolerance are co-ordinated with the leaf phenology of angiosperm trees in an Asian tropical dry karst forest. *Annals of Botany* 110: 189–199.

Giraldo JP, Holbrook NM. 2011. Physiological mechanisms underlying the seasonality of leaf senescence and renewal in seasonally dry tropical forest trees. In: Dirzo R, Young HS, Mooney HA, Ceballos G, eds. *Seasonally dry tropical forests*. Washington, DC, USA: Island Press, 129–140.

Givnish TJ. 2002. Adaptive significance of evergreen vs. deciduous leaves: solving the triple paradox. *Silva Fennica* 36: 703–743.

Ishida A, Harayama H, Yazaki K, Ladpala P, Sasrisang A, Kaewpakasit K, Panuthai S, Staporn D, Maeda T, Gamo M, *et al.* 2010. Seasonal variations of gas exchange and water relations in deciduous and evergreen trees in monsoonal dry forests of Thailand. *Tree Physiology* 30: 935–945.

Javot H, Maurel C. 2002. The role of aquaporins in root water uptake. *Annals of Botany* 90: 301–313.

Klein T. 2014. The variability of stomatal sensitivity to leaf water potential across tree species indicates a continuum between isohydric and anisohydric behaviours. *Functional Ecology* 28: 1313–1320.

Koenker R. 2013. *Quantreg: quantile regression. R package v.5.05*. [WWW document] URL http://CRAN.R-project.org/package=quantreg [accessed 8 September 2014].

Leij FJ, Alves WJ, Van Genuchten MT, Williams JR. 1996. *The UNSODA unsaturated soil hydraulic database user's manual*. Ada, OK, USA: US Environmental Protection Agency National Risk Management Research Laboratory.

Levitt J. 1972. *Responses of plants to environmental stresses*. New York, NY, USA: Academic Press.

Lo Gullo MA, Nardini A, Salleo S, Tyree MT. 1998. Change in root hydraulic conductance (K_R) of *Olea oleaster* seedlings following drought stress and irrigation. *New Phytologist* 140: 25–31.

Lopez OR, Kursar TA, Cochard H, Tyree MT. 2005. Interspecific variation in xylem vulnerability to cavitation among tropical tree and shrub species. *Tree Physiology* 25: 1553–1562.

Machado J-L, Tyree MT. 1994. Patterns of hydraulic architecture and water relations of two tropical canopy trees with contrasting leaf phenologies: *Ochroma pyramidale* and *Pseudobombax septenatum*. *Tree Physiology* 14: 219–240.

Marchin RM, Zeng H, Hoffmann WA. 2010. Drought-deciduous behavior reduces nutrient losses from temperate deciduous trees under severe drought. *Oecologia* 163: 845–854.

Markesteijn L, Poorter L, Paz H, Sack L, Bongers F. 2011. Ecological differentiation in xylem cavitation resistance is associated with stem and leaf structural traits. *Plant, Cell & Environment* 34: 137–148.

McDermitt DK. 1990. Sources of error in the estimation of stomatal conductance and transpiration from porometer data. *HortScience* 25: 1538–1548.

McDowell NG, Fisher RA, Xu C, Domec JC, Hölttä T, Mackay DS, Sperry JS, Boutz A, Dickman L, Gehres N, *et al.* 2013. Evaluating theories of drought-induced vegetation mortality using a multimodel–experiment framework. *New Phytologist* 200: 304–321.

Méndez-Alonzo R, Paz H, Zuluaga RC, Rosell JA, Olson ME. 2012. Coordinated evolution of leaf and stem economics in tropical dry forest trees. *Ecology* 93: 2397–2406.

Munné-Bosch S, Alegre L. 2004. Die and let live: leaf senescence contributes to plant survival under drought stress. *Functional Plant Biology* 31: 203–216.

Nardini A, Battistuzzo M, Savi T. 2013. Shoot desiccation and hydraulic failure in temperate woody angiosperms during an extreme summer drought. *New Phytologist* 200: 322–329.

Nobel PS, Cui M. 1992. Hydraulic conductances of the soil, the root–soil air gap, and the root: changes for desert succulents in drying soil. *Journal of Experimental Botany* 43: 319–326.

Pérez R. 2008. *Árboles de los bosques del Canal de Panamá*. Panama City, Panama: Smithsonian Tropical Research Institute.

Pineda-García F, Paz H, Meinzer FC. 2013. Drought resistance in early and late secondary successional species from a tropical dry forest: the interplay between xylem resistance to embolism, sapwood water storage and leaf shedding. *Plant, Cell & Environment* 36: 405–418.

Powell TL, Galbraith DR, Christoffersen BO, Harper A, Imbuzeiro HMA, Rowland L, Almeida S, Brando PM, da Costa ACL, Costa MH, *et al.* 2013. Confronting model predictions of carbon fluxes with measurements of Amazon forests subjected to experimental drought. *New Phytologist* 200: 350–365.

Reich PB, Borchert R. 1984. Water stress and tree phenology in a tropical dry forest in the lowlands of Costa Rica. *Journal of Ecology* 72: 61–74.

Rosell JA, Gleason S, Méndez-Alonzo R, Chang Y, Westoby M. 2014. Bark functional ecology: evidence for tradeoffs, functional coordination, and environment producing bark diversity. *New Phytologist* 201: 486–497.

Sack L, Tyree MT. 2005. Leaf hydraulics and its implications in plant structure and function. In: Holbrook NM, Zwieniecki MA, eds. *Vascular transport in plants*. Oxford, UK: Elsevier, 93–114.

Schippers JHM, Schmidt R, Wagstaff C, Jing H-C. 2015. Living to die and dying to live: the survival strategy behind leaf senescence. *Plant Physiology* 169: 914–930.

Sobrado MA. 1993. Trade-off between water transport efficiency and leaf life-span in a tropical dry forest. *Oecologia* 96: 19–23.

Sobrado MA. 1997. Embolism vulnerability in drought-deciduous and evergreen species of a tropical dry forest. *Acta Oecologica* 18: 383–391.

Sperry JS, Adler FR, Campbell GS, Comstock JP. 1998. Limitation of plant water use by rhizosphere and xylem conductance: results from a model. *Plant, Cell & Environment* 21: 347–359.

Sperry JS, Donnelly JR, Tyree MT. 1988. A method for measuring hydraulic conductivity and embolism in xylem. *Plant, Cell & Environment* 11: 35–40.

Sperry JS, Hacke UG, Oren R, Comstock JP. 2002. Water deficits and hydraulic limits to leaf water supply. *Plant, Cell & Environment* 25: 251–263.

Sperry JS, Love DM. 2015. What plant hydraulics can tell us about responses to climate-change droughts. *New Phytologist* 207: 14–27.

Sperry JS, Wang Y, Wolfe BT, Mackay DS, Anderegg WRL, McDowell NG, Pockman WT. 2016. Pragmatic hydraulic theory predicts stomatal responses to climatic water deficits. *New Phytologist* 212: 577–589.

Tobin MF, Pratt RB, Jacobsen AL, De Guzman ME. 2013. Xylem vulnerability to cavitation can be accurately characterised in species with long vessels using a centrifuge method. *Plant Biology* **15**: 496–504.

Torres-Ruiz JM, Sperry JS, Fernández JE. 2012. Improving xylem hydraulic conductivity measurements by correcting the error caused by passive water uptake. *Physiologia Plantarum* **146**: 129–135.

Tyree MT, Cochard H, Cruiziat P, Sinclair B, Ameglio T. 1993. Drought-induced leaf shedding in walnut: evidence for vulnerability segmentation. *Plant, Cell & Environment* **16**: 879–882.

Tyree MT, Sperry JS. 1988. Do woody plants operate near the point of catastrophic xylem dysfunction caused by dynamic water stress? Answers from a model. *Plant Physiology* **88**: 574–580.

Tyree MT, Zimmermann MH. 2002. *Xylem structure and the ascent of sap.* Berlin, Germany: Springer-Verlag.

Van Genuchten MT. 1980. A closed-form equation for predicting the hydraulic conductivity of unsaturated soils. *Soil Science Society of America Journal* **44**: 892–898.

Venturas MD, Mackinnon ED, Jacobsen AL, Pratt RB. 2015. Excising stem samples underwater at native tension does not induce xylem cavitation. *Plant, Cell & Environment* **38**: 1060–1068.

Von Allmen AI, Sperry JS, Bush SE. 2015. Contrasting whole-tree water use, hydraulics, and growth in a co-dominant diffuse-porous vs. ring-porous species pair. *Trees – Structure and Function* **29**: 717–728.

Wheeler JK, Huggett BA, Tofte AN, Rockwell FE, Holbrook NM. 2013. Cutting xylem under tension or supersaturated with gas can generate PLC and the appearance of rapid recovery from embolism. *Plant, Cell & Environment* **36**: 1938–1949.

Williams LJ, Bunyavejchewin S, Baker PJ. 2008. Deciduousness in a seasonal tropical forest in western Thailand: interannual and intraspecific variation in timing, duration and environmental cues. *Oecologia* **155**: 571–582.

Wolfe BT, Kursar TA. 2015. Diverse patterns of stored water use among saplings in seasonally dry tropical forests. *Oecologia* **179**: 925–936.

Wright SJ, Cornejo FH. 1990. Seasonal drought and leaf fall in a tropical forest. *Ecology* **71**: 1165–1175.

Wright SJ, van Schaik CP. 1994. Light and the phenology of tropical trees. *American Naturalist* **143**: 192–199.

Zimmermann MH. 1983. *Xylem structure and the ascent of sap.* Berlin, Germany: Springer-Verlag.

Supporting Information

Additional Supporting Information may be found online in the Supporting Information tab for this article:

Fig. S1 Dry season soil water potential during the study period.

Fig. S2 Relationship between measured and predicted leaf area for each study species.

Fig. S3 Twenty-one-month time course of stomatal conductance for each study species.

Fig. S4 Twenty-one-month time course of plant water potential for each study species.

Fig. S5 Stomatal conductance as a function of plant water potential for each study species.

Fig. S6 Modeled vs measured canopy diffusive conductance for each study species.

Fig. S7 Modeled vs measured midday leaf water potential for each study species.

Table S1 Dry season characteristics during the study period

Table S2 Characteristics of saplings used for censuses of leaf area and stomatal conductance

Table S3 Characteristics of stems used for hydraulic conductivity measurements

Table S4 Parameters of Weibull functions used to quantify vulnerability to cavitation

Table S5 Parameters of regression of percentage of November leaf area vs plant water potential

Table S6 Mean absolute errors of hydraulic model outputs

Table S7 Sensitivity of hydraulic model outputs to partitioning of plant organ resistance

Table S8 Hydraulic model parameters that were fitted with iteration

Table S9 Parameters of nonlinear regressions of percentage of November leaf area vs E_{crit}

Table S10 Parameters of nonlinear regressions of $\mathrm{PLC}_{\mathrm{total}}$ vs percentage of November leaf area